

ISFET-based Biosensor Modeling with SPICE

G. MASSOBRIO and M. GRATAROLA

Biophysical and Electronic Engineering Department, University of Genoa, Via all'Opera Pia, 11a, 16145, Genoa (Italy)

G. MATTIOLI

Surgery Department, University of Genoa, Viale Benedetto XV 10, 16132, Genoa (Italy)

F. MATTIOLI, JR.

Medical Pharmacology, University of Genoa, Viale Benedetto XV 1, 16132, Genoa (Italy)

Abstract

An ISFET model suitable for direct applications as a built-in model in SPICE, is presented. The ISFET 'static' model equations are formulated by modifying the MOST threshold voltage which, for the ISFET, is chemically influenced by ionic interaction between the electrolyte and the insulator. The ISFET 'large-signal model' has been obtained from the site-binding model of the insulator–electrolyte interface, combined with the Gouy–Chapman–Stern theory of the electrical double layer at this interface, varying the Meyer's large-signal model of the MOST in SPICE. The proposed model leads to the introduction of twelve new parameters that the user of SPICE can specify in the .MODEL card. For these parameters the temperature dependence has also been implemented. The model has been used to simulate the output characteristics of Ag/AgCl–KCl–SiO₂–Si and Ag/AgCl–NaCl–Al₂O₃–SiO₂–Si ISFET structures at different pH values, and ISFET-based circuits, obtaining a good agreement with experimentally measured values.

Introduction

The structure of the ion-selective field-effect transistor (ISFET) [1] is essentially a MOST [2] which can be rendered ion-sensitive by eliminating its metal gate electrode in order to expose the gate insulator to the solution. The gate insulator or ion-selective membrane senses the specific ion concentration, generating an interface potential on the gate; the corresponding drain-source current change in the semiconductor channel is observed. From a comparison of MOST (Fig. 1) and ISFET (Fig. 2) structures, it is apparent that the only difference between the electrical circuits is the replacement of the metal gate of the MOST by the series combination of the reference electrode, elec-

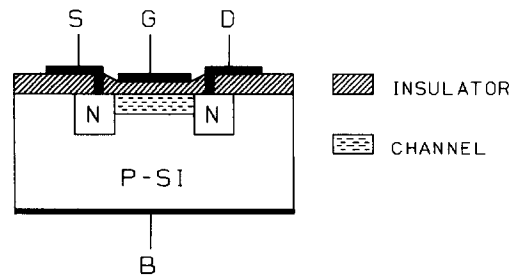


Fig. 1. Schematic representation of the MOST.

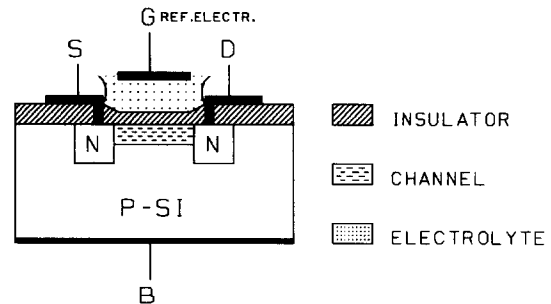


Fig. 2. Schematic representation of the ISFET.

trolyte and chemically sensitive insulator or membrane.

In the following sections, the ISFET model (pointing out the difference with the MOST), its implementation in SPICE [3] and its simulation in ISFET-based circuits are presented.

ISFET Model

Static Model

The equations describing the operation of the ISFET can be derived from the analogous equations of the MOST by taking into account the potential differences among the new elements in the circuit.

For the conventional MOST device, the relationship between drain current I_d , the drain-source voltage V_{ds} , gate-source voltage V_{gs} , and the device threshold voltage V_{th} , is given by the expressions [2]

$$I_d = (\beta/2)(V_{gs} - V_{th})^2 \quad (1)$$

(saturation region)

$$I_d = \beta[(V_{gs} - V_{th}) - V_{ds}/2]V_{ds} \quad (2)$$

(linear region)

where $\beta = \mu C_{ox} W/L$, μ = charge carrier mobility in the channel, C_{ox} = insulator capacitance per unit area, W = channel width, L = channel length. The threshold voltage V_{th} is determined by the properties of the semiconductor materials and fabrication process, and is given by [2]

$$V_{th}(\text{MOST}) = \phi_{ms} + 2\phi_f - (Q_{ss} + Q_{sc})/C_{ox} \quad (3)$$

where ϕ_{ms} = metal-semiconductor work function difference, ϕ_f = Fermi potential of the semiconductor (p-type for the n-channel MOST here considered), Q_{ss} = fixed surface-state charge density per unit area at the insulator-semiconductor interface, and Q_{sc} = semiconductor surface depletion region charge per unit area. Q_{ss} and Q_{sc} are considered independent of chemical activity in the electrolyte [4]. Equations (1) through (3) define the so-called MOST static model.

In order to adapt eqns. (1) and (2) to the ISFET structure, new expressions for V_{gs} and V_{th} must be established. If all the potential terms in the ISFET configuration are included in the definition of the ISFET threshold voltage V_{th} , the interface potentials generated by the reference electrode and the chemical insulator or membrane in the solution (that contribute to the new expression of V_{gs}) are also included in V_{th} to give [4-6].

$$V_{th}^*(\text{ISFET}) = (E_{ref} + \phi_{ij}) - (\phi_{eo} - X_{eo}) - [(Q_{ss} + Q_{sc})/C_{ox} - 2\phi_f + (\phi_s/q)] \quad (4)$$

Terms common to eqns. (3) and (4), such as Q_{ss} , Q_{sc} , ϕ_f and C_{ox} , retain their conventional definitions according to the standard MOST theory, while E_{ref} = potential of the reference electrode, ϕ_{ij} = liquid junction potential difference between reference solution and the electrolyte, ϕ_{eo} = potential of electrolyte-insulator interface, X_{eo} = electrolyte-insulator surface dipole potential, and ϕ_s/q = semiconductor work function. In particular, for the considered n-channel ISFET with a Ag/AgCl reference electrode, we may write

$$E_{ref} = E_{abs}(H^+/H_2) + E_{rel}(\text{Ag}/\text{AgCl}) \quad (5)$$

where $E_{abs}(H^+/H_2)$ = potential of the standard hydrogen electrode, and $E_{rel}(\text{Ag}/\text{AgCl})$ =

potential of Ag/AgCl reference electrode (relative to the hydrogen electrode).

Equation (4) contains terms common to the standard MOST theory, as well as terms that are electrochemical in nature. The most important of these is the potential ϕ_{eo} , which determines the sensitivity of the ISFET to specific chemical species. In general, ϕ_{eo} is determined by the surface reaction between ions in solution and reactive sites on the insulator surface. By considerations of the equilibrium reactions between the insulator surface sites and species in solution which they complex, it is possible to derive expressions which relate the interfacial potential ϕ_{eo} to the activity of the potential-determining species (primarily H^+). The derivations are based on the site-binding model combined with the Gouy-Chapman-Stern theory of the double layer at the electrolyte-insulator interface. For a simple univalent electrolyte, using the approximations introduced in ref. 7, the pH response of a single-site unit surface is

$$2.303(\text{pH}_{pzc} - \text{pH}) = (q\phi_{eo}/kT) + \sinh^{-1}[(q\phi_{eo})/(\beta^*kT)] \quad (6)$$

in which β^* is a dimensionless parameter that characterizes the pH sensitivity of the insulator.

For a single-site system [7]

$$\beta^* = (2q^2 N_{bs}) / [(kTC_{dl})(K_a/K_b)^{0.5}] \quad (7)$$

with

$$\text{pH}_{pzc} = -\log_{10}(K_a K_b)^{0.5} \quad (8)$$

In eqns. (6) and (7), kT/q = thermal voltage, N_{bs} = density of binding sites per unit area on the insulator surface, C_{dl} = double layer capacitance per unit area, K_a = acidic dissociation constant, K_b = basic dissociation constant, pH_{pzc} = pH value at the point of zero charge.

By comparing eqns. (3) and (4) we may write

$$V_{th}^*(\text{ISFET}) = V_{th}(\text{MOST}) + \Delta V_{th}^* \quad (9)$$

where we have introduced

$$\Delta V_{th}^* = E_{ref} + \phi_{ij} + X_{eo} - \phi_{eo} - \phi_m/q \quad (10)$$

that represents the ISFET threshold voltage component depending on the sensitivity of the device, and ϕ_m/q = work function of the metal gate (reference electrode) relative to vacuum. If in eqns. (1) and (2), the MOST threshold voltage V_{th} is replaced by V_{th}^* , we obtain the ISFET static model.

Large-signal Model

The ISFET large-signal model is based on the MOST large-signal model, characterized by two pn junction depletion layer capacitances, C_{bs} and C_{bd} , and by the gate-source, gate-drain, gate-bulk

capacitances, C_{gs} , C_{gd} and C_{gb} respectively, which in their turn are a function of the insulator capacitance C_{ox} . For the ISFET, the capacitance C_{ox} is sensitive to the ionic activity of the electrolyte and it consists of two elements connected in series: the MOST insulator capacitance C_{ox} and the double layer capacitance C_{dl} . Thus to model the large-signal behavior of the ISFET it is necessary to consider

$$C_{ox} = C_{ox} C_{dl} / (C_{ox} + C_{dl}) \quad (11)$$

Thermal Model

The strong similarity of the MOST and ISFET can be exploited in the analysis of the temperature dependency of the ISFET. Because both drain current eqns. (1) and (2) depend only on the quantities β , V_{th} and applied voltages, any temperature dependence must be through the quantities β and V_{th} .

In the next three subsections we shall take into account each of the terms in β and V_{th} parameters in regard to their temperature dependences.

Semiconductor terms

The mobility μ of carriers in the channel is an inverse function of absolute temperature T according to the following empirical expression

$$\mu(T) = \mu(300)(300/T)^a \quad (12)$$

where temperature T is in Kelvin and the exponent a is between 1.0 and 1.5.

The Fermi potential ϕ_f can be expressed as

$$\phi_f = (kT/q) \ln(N/n_i) \quad (13)$$

where N is the ionized impurity density (assumed equal to the impurity atom density). In addition, the intrinsic electron density n_i is assumed to be given by

$$n_i = BT^{1.5} \exp(-qE_g(0)/2kT) \quad (14)$$

where B is a constant independent of T , and $E_g(0)$ is the energy gap at 0 K whose dependence on temperature is

$$E_g(T) = E_g(0) - (\alpha T^2)/(\gamma + T) \quad (15)$$

For silicon, $\alpha = 7.02 \times 10^{-4}$, $\gamma = 1108$, and $E_g(0) = 1.16$ eV.

The fixed surface-state charge density Q_{sc} , for a uniformly doped substrate, is temperature-dependent through ϕ_f according to the relation

$$Q_{sc} = (2\epsilon_s q N (2\phi_f))^{0.5} \quad (16)$$

where ϵ_s is the semiconductor dielectric constant.

Reference electrode terms

The reference electrode assumed is a Ag/AgCl electrode with filling solution of 3.5 M KCl, satu-

rated with AgCl. From eqn. (5), we can write the temperature dependence of the reference electrode potential E_{ref} of this type of electrode as [8]

$$\begin{aligned} E_{ref}(T) &= E_{abs}(H^+/H_2) + E_{rel}(Ag/AgCl) \\ &\quad + (dE_{ref}/dT)(T - 298.16) \\ &= 4.7 + 0.205 + 1.4 \times 10^{-4}(T - 298.16) \end{aligned} \quad (17)$$

The liquid-junction potential ϕ_{lj} is typically quite small (a few millivolts), thus its dependence on temperature is insignificant in comparison to that of any other temperature-dependent term [8]. We therefore remove this term from further considerations.

Insulator-electrolyte interface terms

The temperature dependence of the electrolyte-insulator potential ϕ_{eo} depends on β^* terms. The most important of these are the dissociation constants K_a and K_b that depend on temperature according to the relation

$$K_{a,b}(T) = K(300)^{300/T} \quad (18)$$

while the other terms of eqn. (7) seem to be independent of temperature [8].

The electrolyte surface dipole potential X_{eo} is a function of both temperature and electrolyte composition. In particular

$$\begin{aligned} X_{eo}(T) &= 50 \times 10^{-3} [1 - \exp(-0.86pI)] \\ &\quad \times [1 - 0.008(T - 298.16)] \end{aligned} \quad (19)$$

where $pI = -\log_{10}(FI)$, FI being the ionic strength. Equations (12) through (19) define the ISFET thermal model.

ISFET Model in SPICE

Static Model

The equations describing the MOST static model [9, 10] in the MOSFET subroutine of SPICE have been kept for the ISFET static model, by replacing the expression of V_{th} of the MOST with eqns. (9) and (10). The pH sensitivity of the insulator has been taken into account implementing eqns. (6) and (7). Thus, in addition to the MOST static model parameters of SPICE, we have introduced nine parameters that the user of SPICE can specify in the .MODEL card [11] to model the static behavior of the ISFET. These parameters are: E_{rel} , X_{eo} , ϕ_{lj} , ϕ_m , N_{bs} , K_a , K_b , C_{dl} and pH_{pzc} . Finally, in order to simulate ISFET devices with more than one insulator layer (in fact SPICE has only built-in parameters for SiO₂-type insulator), we have introduced two new parameters for the .MODEL card: the added insulator thickness t_{oxl} and its dielectric constant ϵ_{oxl} .

Large-signal Model

The equations describing the MOST large-signal model [9, 10] in the CMEYER subroutine of SPICE have been kept for the ISFET large-signal model, by replacing the insulator capacitance C_{ox} of the MOST with eqn. (11). Thus, to characterize the ISFET large-signal model behavior, the user of SPICE has to specify the C_{dl} parameter in the .MODEL card [11].

Thermal Model

As regards the temperature dependence, the parameters common to the MOST and ISFET structures retain their definition [9, 10] in the TMPUPD subroutine of SPICE. Therefore, only eqns. (17) through (19) have been implemented in SPICE to define the thermal model of the ISFET by introducing a new parameter for the .MODEL card [11]: the ionic strength FI .

Simulation Results

The validity of the ISFET model has been investigated for Ag/AgCl-KCl-SiO₂-Si and Ag/AgCl-NaCl-Al₂O₃-SiO₂-Si structures with the

basic parameter values specified in the .MODEL cards as shown in Fig. 3. Other fundamental quantities relative to the MOST model and not specified in the .MODEL card, such as the threshold voltage, the surface potential and the transconductance parameter, are automatically computed in SPICE by the geometric and process parameters as described in refs. 9 and 10.

Figure 4 shows the static characteristics (obtained from simulation with SPICE) for the two ISFET structures at two different pH values; for comparison we have added the characteristics of a MOST with the same technological properties as the ISFETs. Figures 5, 6 and 7 represent SPICE simulation results of ISFET static characteristics obtained by varying the oxide thickness, the surface binding site density and the temperature, respectively.

Once the ISFET static behavior has been investigated, we have simulated the circuit of Fig. 8. Such a circuit is known as [12] 'operational transducer': a matched (Ag/AgCl-KCl-SiO₂-Si) ISFET/MOST pair is connected in source-coupled dual-differential configuration and the output voltages are coupled to a differential/single-ended converter and to a d.c. amplification stage such that the ISFET is the non-inverting input device,

```

*
.MODEL isfNaCl NMOS LEVEL=4 TOX=100N LD=0.8U XJ=1U NSUB=5.E16
+ TPG=1 UO=750 RD=5 RS=5 LAMBDA=0.02 NSS=1.E11
+ XQC=1 IS=1F CGSO=275P CGDO=275P CGBO=200P
+ PB=0.88 CJ=700U MJ=0.5 CJSW=80N MJSW=0.33
+ tox1=50n epsox1=66.6p
+ erel=0.205 phpzc=8.6 phim=4.30 chieo=3.e-3
+ akappa=2u bkappa=3.16p philj=3.e-3
+ xnbs=8.e14 cdl=20u fi=0.1
*
.MODEL isfKCl NMOS LEVEL=4 TOX=100N LD=0.8U XJ=1U NSUB=5.E16
+ UO=750 RD=5 RS=5 LAMBDA=0.02 TPG=1 NSS=1.E11
+ XQC=1 IS=1F CGSO=275P CGDO=275P CGBO=200P
+ PB=0.88 CJ=700U MJ=0.5 CJSW=80N MJSW=0.33
+ erel=0.205 phpzc=2.5 phim=4.30 chieo=3.e-3
+ akappa=31.6 bkappa=3.16e-7 philj=3.e-3
+ xnbs=5.e14 cdl=20u fi=0.1
*
.MODEL most NMOS LEVEL=2 TOX=100N LD=0.8U NSUB=5.E16 NSS=1.E11
+ UO=750 RD=5 RS=5 LAMBDA=0.02 TPG=1
+ XQC=1 IS=1F CGSO=275P CGDO=275P CGBO=200P
+ PB=0.88 CJ=700U MJ=0.5 CJSW=80N MJSW=0.33
*-----*
M1SPD 22 1 0 0 isfNaCl L=10U W=50U PH=2. AD=100P AS=100P PS=40U PD=40U
M3SPD 42 1 0 0 isfNaCl L=10U W=50U PH=12. AD=100P AS=100P PS=40U PD=40U
M4SPD 52 1 0 0 isfKCl L=10U W=50U PH=2. AD=100P AS=100P PS=40U PD=40U
M6SPD 72 1 0 0 isfKCl L=10U W=50U PH=12. AD=100P AS=100P PS=40U PD=40U
*
Mtest 23 1 0 0 most L=10U W=50U AD=100P AS=100P PS=40U PD=40U
*

```

Fig. 3. SPICE input for the simulation of ISFET static characteristics, pointing out ISFET model parameters (in lower case).

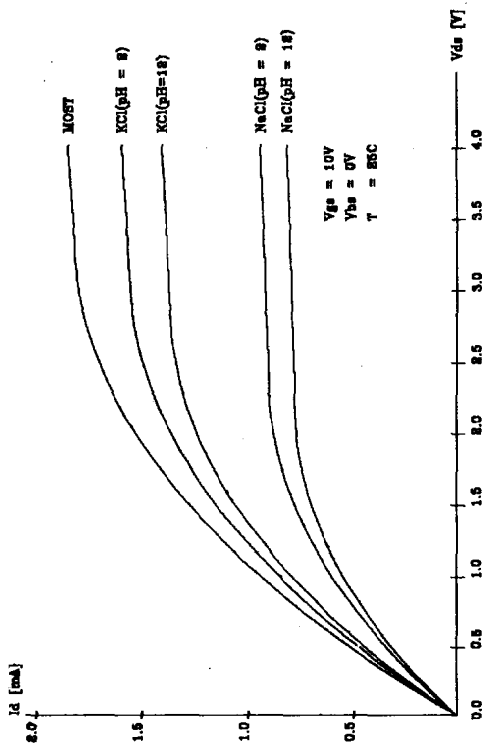


Fig. 4. ISFET static characteristics obtained from SPICE simulation by using input parameters of Fig. 3.

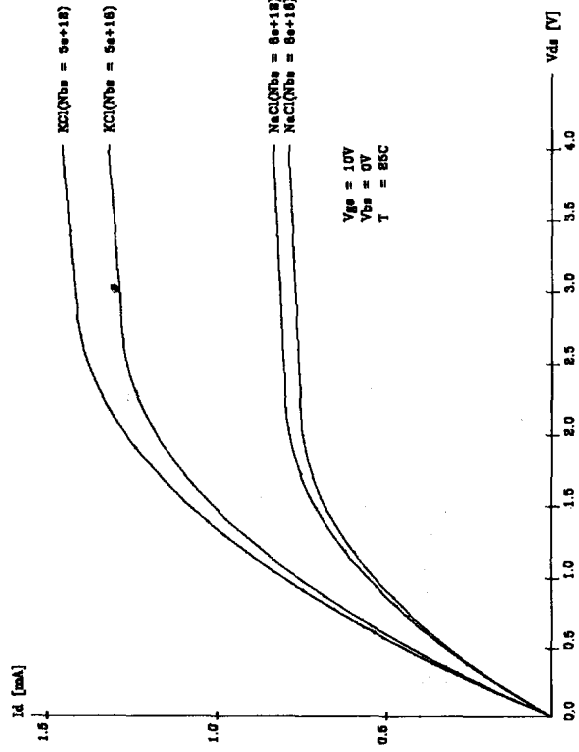


Fig. 6. ISFET static characteristics obtained from SPICE simulation by varying N_{bs} parameter at pH = 12. (The other ISFET model parameters are those of Fig. 3.)

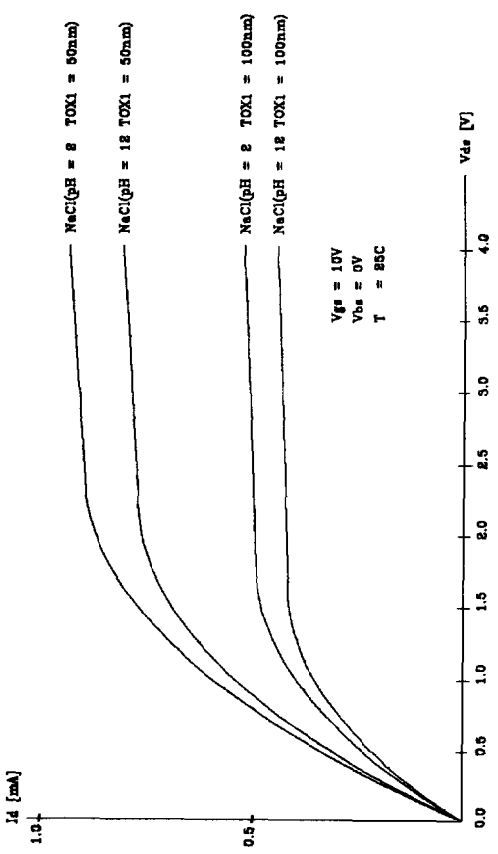


Fig. 5. ISFET static characteristics obtained from SPICE simulation by varying τ_{ox1} parameter at two different pH values. (The other ISFET model parameters are those of Fig. 3.)

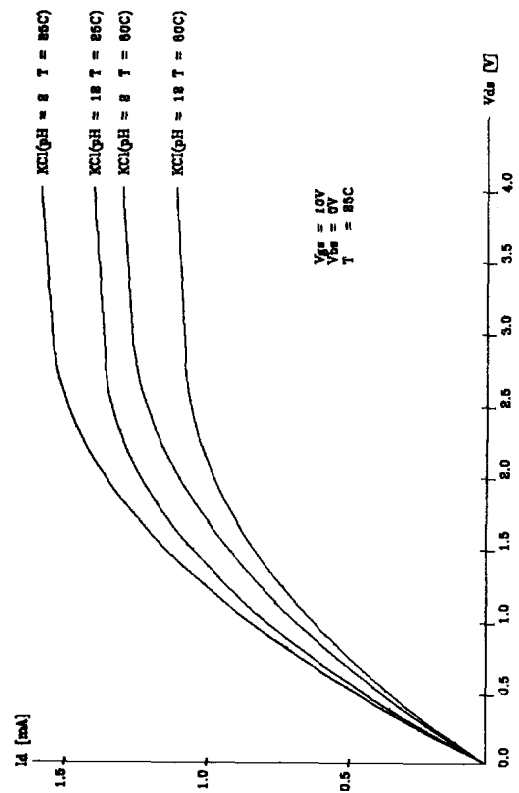


Fig. 7. ISFET static characteristics obtained from SPICE simulation by varying T parameter at two different pH values. (The other ISFET model parameters are those of Fig. 3.)

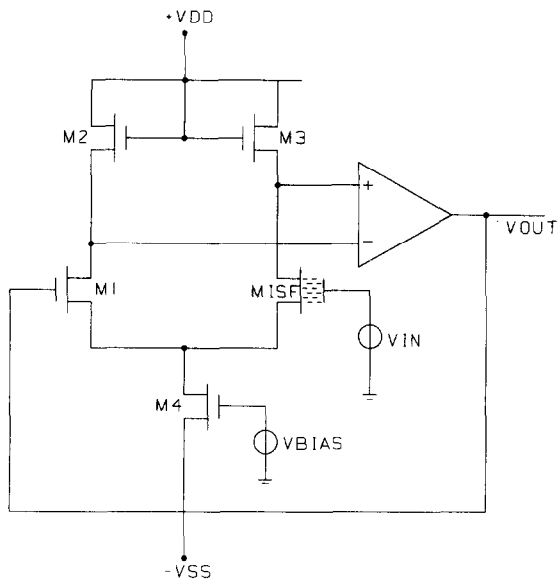


Fig. 8. Operational transducer circuit.

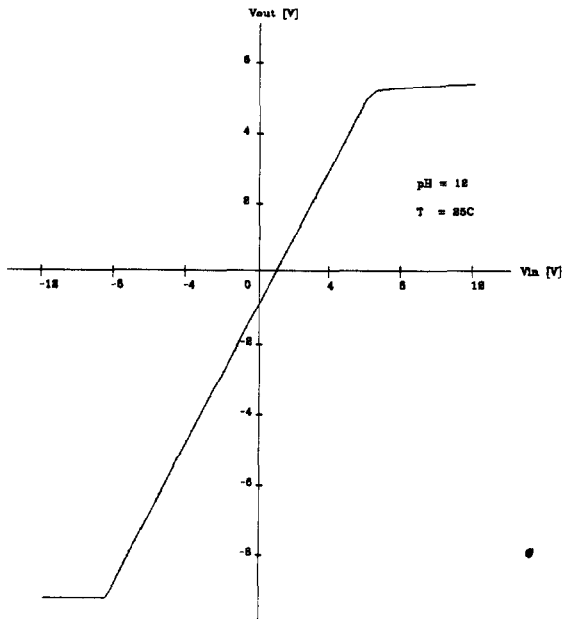


Fig. 9. Transfer characteristics of the circuit of Fig. 8 obtained from SPICE simulation. (The ISFET model parameters are those of Fig. 3.)

and the MOST is the inverting input device. The transfer characteristics of the circuit (in this instance, a pH-responsive transducer), are shown in Fig. 9. Then, the pH has been swept in the range pH 2 to pH 12 to evaluate the pH response of the circuit: the electrochemical characteristics we have obtained from SPICE simulation are shown in Fig. 10, pointing out the dependence of the output voltage on pH.

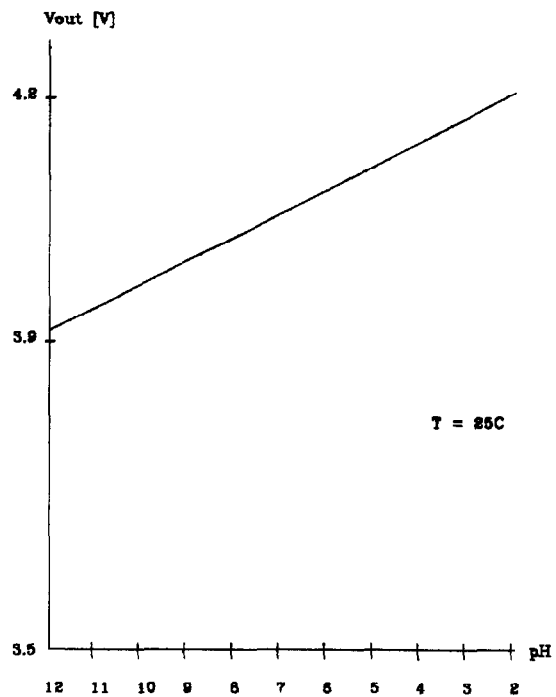


Fig. 10. Chemical characteristics of the circuit of Fig. 8 obtained from SPICE simulation. (The ISFET model parameters are those of Fig. 3.)

Discussion and Conclusions

The results presented here show that the proposed ISFET model implemented in SPICE well simulates ISFET behavior both as a discrete structure and as a component in circuit operation. Besides the advantages typical of CAD techniques, the availability of an ISFET model in the most widely used electronic simulation program, such as SPICE, allows the electronic circuit designer to also incorporate, from now on, ISFETs in the simulation of electronic circuitry for equipments containing these devices. The model, defined by twelve parameters besides the ones of the MOST, takes into account the first-order effects of the ISFET. The next step we are working on is to implement the second-order effects to simulate ISFETs with electroactive materials for measurements of different species.

Acknowledgements

The authors wish to thank Dr E. Meda for many valuable discussions. This work is partially supported by the National Research Council (CNR) of Italy, Progetto Finalizzato 'Materiali e Dispositivi per l'Elettronica a Stato Solido'.

References

- 1 P. Bergveld, Development of an ion-sensitive solid state device for neurophysiological measurements, *IEEE Trans. Biomed. Eng.*, *BME-17* (1970) 70–71.
- 2 D. Witt and G. Ong, *Modern MOS Technology*, McGraw-Hill, New York, 1984.
- 3 W. Nagel, *SPICE2*, a computer program to simulate semiconductor circuits, *ERL-M520*, Electronics Research Laboratory, University of California, Berkeley, CA, 1975.
- 4 S. D. Moss, C. C. Johnson and J. Janata, Hydrogen, calcium and potassium ion-sensitive FET transducer: a preliminary report, *IEEE Trans. Biomed. Eng.*, *BME-25* (1978) 49–54.
- 5 L. Bousse, Single electrode potentials related to flat-band voltage measurements on EOS and MOS structure, *J. Chem. Phys.*, *76* (1982) 5128–5133.
- 6 L. Bousse, N. F. de Rooij and P. Bergveld, Operation of chemically sensitive field-effect sensors as a function of the insulator–electrolyte interface, *IEEE Trans. Electron Devices*, *ED-30* (1983) 1263–1270.
- 7 D. L. Harame, L. J. Bousse, J. D. Shott and J. D. Meindl, Ion-sensing devices with silicon nitride and borosilicate glass insulators, *IEEE Trans. Electron Devices*, *ED-34* (1987) 1700–1707.
- 8 P. Barabash, R. S. C. Cobbold and W. B. Wlodarski, Analysis of the threshold voltage and its temperature dependence in electrolyte–insulator–semiconductor field-effect transistors (EISFETs), *IEEE Trans. Electron Devices*, *ED-34* (1987) 1271–1282.
- 9 P. Antognetti and G. Massobrio, *Semiconductor Device Models with SPICE*, McGraw-Hill, New York, 1988.
- 10 G. Massobrio, *Modelli dei Dispositivi a Semiconduttore in SPICE*, F. Angeli, Milan, 1986.
- 11 *SPICE2 User's Guide*, Electronics Research Laboratory, University of California, Berkeley, 1981.
- 12 A. Sibbald, A chemical-sensitive integrated-circuit: the operational transducer, *Sensors and Actuators*, *7* (1985) 23–38.